

Evaluation of Drag and Lift Forces of Grooved Cylinders in Wind Tunnel

Aiman N.N. * and Samion S.

School of Mechanical Engineering, Faculty of Engineering,
Universiti Teknologi Malaysia,
81310 UTM Johor Bahru,
Johor, Malaysia

*Corresponding email: naimaiman@hotmail.com

Article history

Received
13 December 2019
Revised
1 April 2020
Accepted
25 May 2020
Published
15 June 2020

ABSTRACT

It is shown that surface modifications on surface of a circular cylinder affects the separation point to move backward on the cylinder surface hence reducing the drag coefficient. The flow past a circular cylinder with smooth, half and full rectangular grooved surface (roughness coefficient $k/D = 0.004$) was investigated in a low speed open end wind tunnel. The outer diameter(D) of the cylinders is 50mm and the depth(k) of the groove is 2mm. The Reynolds number used in the study ranges from 1.65×10^4 to 1.13×10^5 . The drag and lift coefficients of the cylinders were measured using a three-component balance. The wake flow pattern of the cylinders was observed based on a smoke visualization technique. The results showed that the full-grooved cylinder and the half-grooved cylinder facing the flow (front) produce lower drag compared to a smooth cylinder and half-grooved cylinder located at the leeside of the flow (rear). The presence of the grooves on the cylinder surface affects the boundary layer and shows a smaller and narrower wake compared to a smooth cylinder.

Keywords: Flow around cylinder, grooved cylinder, Reynolds number, smoke visualization, wind tunnel test

1.0 INTRODUCTION

Cylindrical structures are prevalent and widespread in many real-world applications, particularly those related to offshore and marine engineering fields including the construction of marine pipe lines, jacket, and jack up and tension-leg platforms. They can be found in various structural designs like flow around chimney stacks, long span bridges, tall buildings, towers, cables, etc. Circular cylinder structure produces large drag due to the pressure difference between the upstream and downstream direction of the flow [1]. Therefore, drag reduction has been the main theme in a number of investigations including this research.

Drag force is the force that acts on an object to resist its motion through a fluid drag coefficient, commonly denoted in fluid dynamics as C_D . The drag coefficient is a non-dimensional quantity computed from the total pressure over the platform area and then normalized by the dynamic pressure. The drag force is the net force exerted by a fluid on a body subjected to a flow due to the combined effects of the wall shear and pressure forces.

Drag reduction of an object is influenced by the shape and surface of the object. Objects with different surfaces will correspondingly produce different values of the drag coefficients.

Based on the superposition of basic potential flows in ideal flow theory, the combination of doublet and the uniform flow is used to resemble the flow over a cylinder. Doublet on the other hand is the combination of sink and source flow at the same time and location. A radially symmetrical flow field directed outwards from a common point is called a source flow while sink is the opposite of source. The streamlines are radial, directed inwards to the line source.

The flow behavior around the cylinder are related to the *Reynolds* number. The *Reynolds* number is the ratio of inertial forces to viscous forces and is a convenient parameter for predicting if a flow condition will be laminar or turbulent and *Re* is defined as in Equation (1):

$$Re = \frac{\rho U D}{\mu} \quad (1)$$

Where *Re*, ρ , *U*, *D* and μ are the *Reynolds* number, density of air, speed, cylinder diameter and kinematic viscosity, respectively.

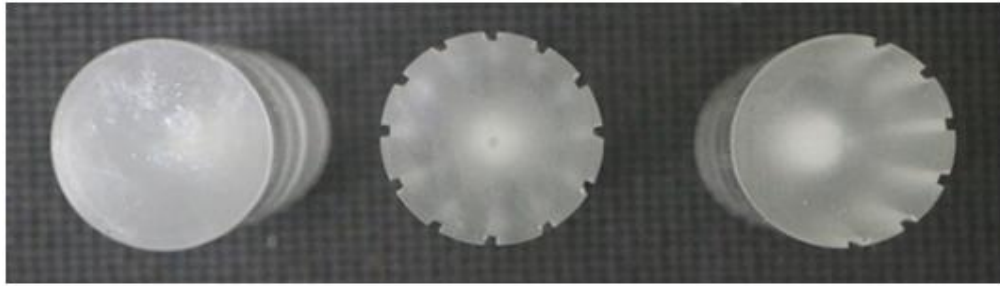
When the *Reynolds* numbers are small ($Re \lesssim 1$) the flow is called creeping flow and there is no separation. The drag is all due to skin friction. As the *Reynolds* number is increased, the drag decreases and there is a separation of boundary layer. The separation starts to occur at around $Re \cong 10$ while vortex shedding occurs at about $Re \cong 90$. Two rows of vortices are formed called the *Vortex Street* on the leeward side of the cylinder. In moderate *Reynolds* number range of $10^3 \lesssim Re \lesssim 10^5$, flow in boundary layer is laminar while the flow behind the separation region is highly turbulent with wide turbulent wake. Meanwhile when the value for *Reynolds* number exceeds 10^5 , the flow becomes turbulent and the separation point slowly moves further hence narrowing the wake size.

Passive flow control methods require no auxiliary power and no control loop. Passive control technique normally involves surface modifications through the addition of extra devices. Instead of adding devices, modifications on the cylinder surface texture could also lead to a good vortex suppression and drag reduction. The modifications of surface texture includes sand roughened surfaces [2], dimples [3-5] and grooves [4, 6, 7]. These studies showed that the acting forces on a cylinder could be modified through surface modifications.

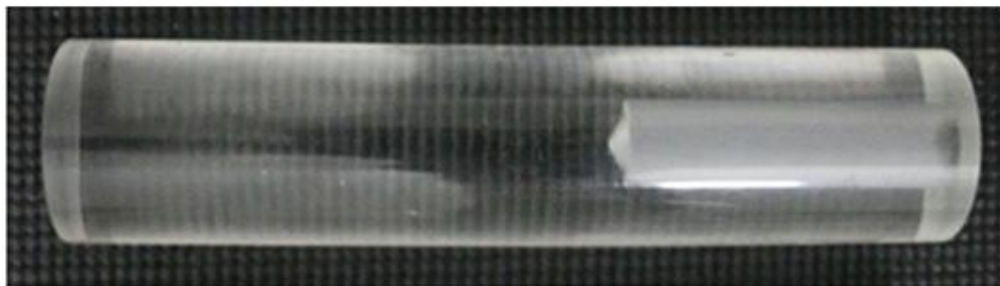
The groove surface roughness modification including dimples are examples of the grooved patterns that has been used as an effective measure for drag reduction [4]. Grooves are depressions cut on the cylinder curved surface. It can be in different shapes and forms, including V-shape [6, 8], U-shape [7-9] and rectangular shape [4, 10]. The orientation of the grooves on the cylinder surface are also dependent on their configurations or types. There are three known orientation types which are the circumferential ring type [11], helical type [12] and longitudinal type [4, 6, 8].

2.0 METHODOLOGY

For this research, a circular cylinder with different surfaces has been used as the test model specimen. Three acrylic rods with a length of 190 mm and final diameter of 50 mm have been utilized as the circular cylinder object of interest as shown in Figure 1b. There are three types of surface used for the test which are smooth, grooves on half surface of cylinder (front and rear) and grooves on a full cylinder as shown in Figure 1a. The grooves were machined based on a longitudinal orientation type and also spaced equally along the circle circumference. The full-grooved cylinder has 12 grooves covering the whole circular circumference while the half-grooved cylinder has six equally spaced grooves covering only half of the circular circumference. The cross-section design of the grooved cylinder is shown in Figure 2. The width and depth of the grooves are 3mm and 2mm, respectively.



(a)



(b)

Figure 1: (a) Types of different surfaces on the test models from top (b) smooth acrylic rod

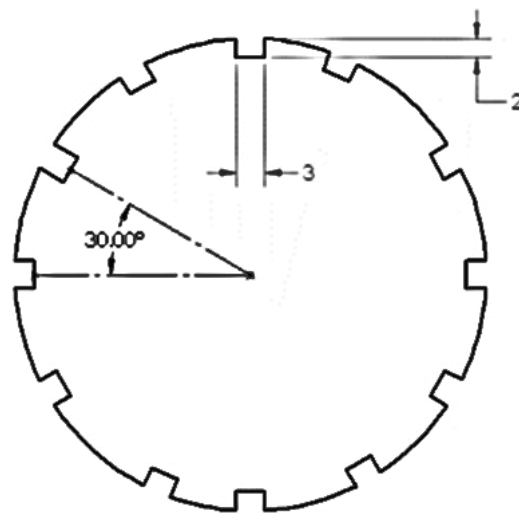


Figure 2: Cross-section design of the grooved cylinder

For the half-grooved cylinder surface, two orientations were applied with the grooves located on the front side and the lee side (rear) of the cylinder. The drag coefficient and smoke visualization tests were conducted using the low speed wind tunnel. The drag coefficient test was conducted at seven different speeds according to 5.2, 8.4, 10.6, 15.4, 20.5, 25.5, 30.5 and 35.5 m/s for each type and orientation of the cylinders. The drag coefficient, C_D from the experiment was used to calculate the drag force for each cylinder using Equation (2):

$$F_D = C_D \frac{1}{2} \rho A V^2 \quad (2)$$

Where F_D is the drag force in N, A is the projected area of the cylinder exposed to the flow, ρ and V are the density and free stream velocity of the flow, respectively. The projected area, A of the cylinder was calculated by multiplying the length with the diameter of the cylinder.

The lift coefficient, C_L on the other hand was used to calculate the lift force, F_L as shown in Equation (3):

$$F_L = \frac{C_L \rho A V^2}{2} \quad (3)$$

The smoke visualization test was conducted at a constant speed of 1.5 m/s and the flow behavior and separation point of the cylinders were observed. To generate the flow pattern around cylinder, the 1500W fog machine was used and the observation results were recorded with a *Canon E70 DSLR* camera.

3.0 RESULTS AND DISCUSSION

The experiment was conducted in a low speed wind tunnel for the drag and lift coefficient tests while a smoke visualization technique was used for the flow visualization test.

3.1 Drag and Lift Coefficients

The drag and lift coefficient tests were performed on every types of cylinders having smooth surface, full-grooved surface, grooves on front half surface (front) and grooves on rear half surface (rear) of the cylinders. The drag coefficient results are shown in Table 1 while those of the lift coefficient shown in Table 2. The trend of the results can be seen clearly in Figure 3 where the smooth and half-grooved surface (rear) produce the highest drag coefficient while the other two cylinders showed a lower drag coefficient value. It can be seen that the graph trends for all the cylinders indicate that the drag coefficient decreases as the speed increases. This shows that the presence of grooves is effective in reducing the drag coefficient of the cylinders especially at low speeds.

Table 1: Drag coefficient results

Velocity (m/s)	Drag coefficient			
	Smooth cylinder	Half-grooved (Front)	Half-grooved (Rear)	Full- grooved
5.2	3.4528	2.0079	2.5310	0.7224
8.4	1.2742	0.7536	0.9731	0.2552
10.6	0.7562	0.4448	0.5995	0.1187
15.4	0.3573	0.3229	0.2522	0.1356
20.5	0.2169	0.1970	0.1971	0.1552
25.5	0.1713	0.1280	0.1709	0.1030
30.5	0.1506	0.1070	0.1481	0.0607
35.5	0.1258	0.0960	0.1302	0.0572

Based on Figure 3, the drag coefficients C_D for all cylinders decrease as the *Reynolds* number increases. According to [13], the drag coefficient decreases with increasing *Reynolds* number. As the *Reynolds* number increases, the boundary layer changes, which in turn moves the separation point further on the rear body, thereby reducing the wake

size. Thus, the magnitude of the pressure drag is reduced. The groove increases the surface roughness and causes the boundary layer to become turbulence at lower *Reynolds* number. Hence, delaying the separation and narrowing the wake reduce the pressure drag considerably.

Table 2: Lift coefficient results

Velocity (m/s)	Lift coefficient			
	Smooth cylinder	Half-grooved (Front)	Half-grooved (Rear)	Full-grooved
5.2	3.8347	0.5281	0.5547	3.3066
8.4	1.5020	0.2139	0.2189	0.6345
10.6	0.9672	0.1299	0.1307	0.8401
15.4	0.4634	0.2795	0.0625	0.4789
20.5	0.2770	0.1804	0.1025	0.1931
25.5	0.2186	0.1174	0.1164	0.1817
30.5	0.2072	0.1021	0.1237	0.0895
35.5	0.1856	0.0935	0.1518	0.0903

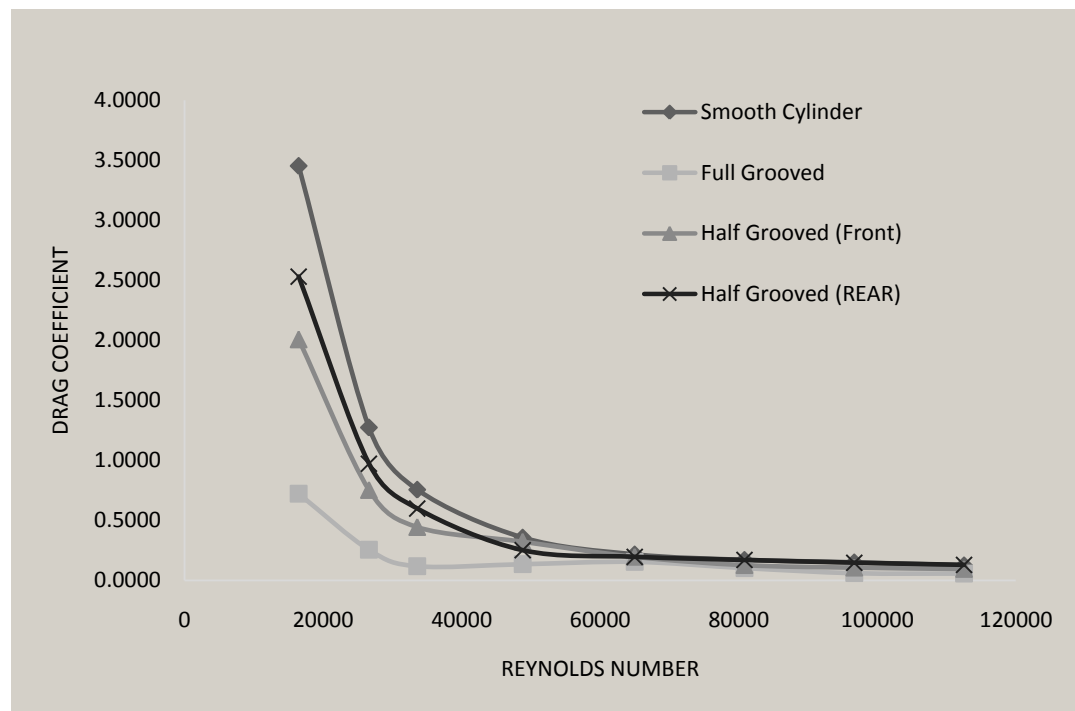


Figure 3: Graphs of the drag coefficient against *Reynolds* number

From Figure 4, the coefficient values are considerably affected by the groove patterns as well as the orientation of the grooved surface with respect to the incident flow. The lift force on the cylinder periodic vortex shedding from the cylinder apparently fluctuates at a certain velocity, which corresponds to the periodic vortex shedding from the cylinder[4]. Spherical or cylindrical form produces zero lift due to top-bottom symmetry[14].

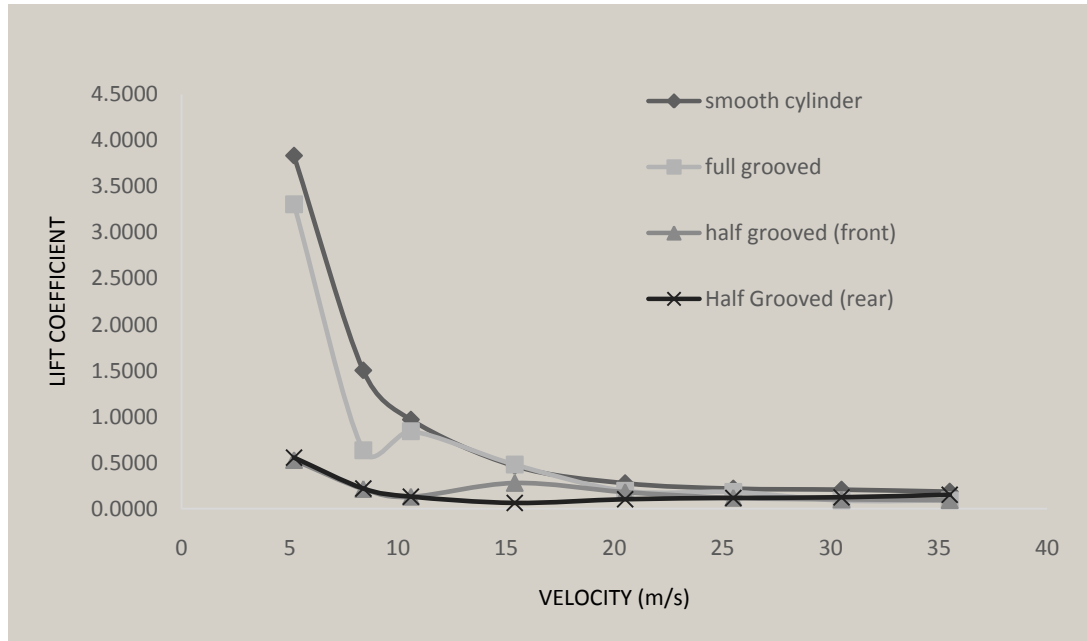
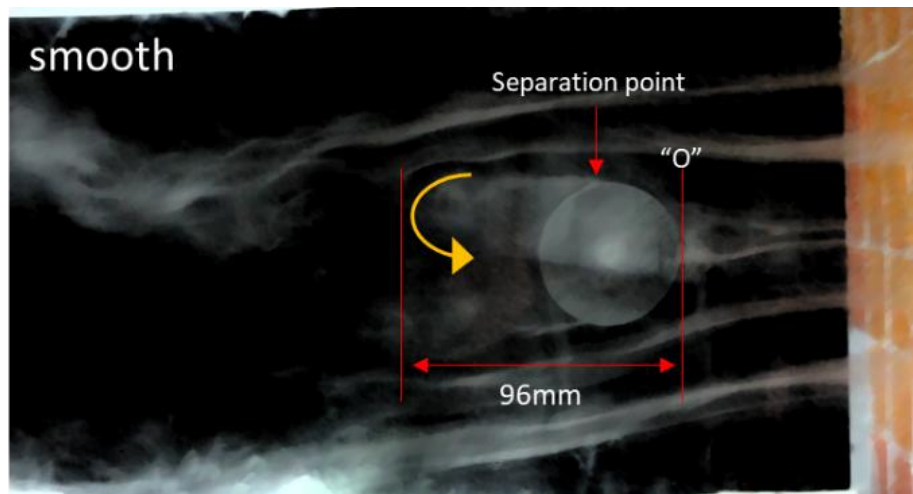


Figure 4: Graphs of the lift coefficient against velocity

3.2 Flow Visualization Test

To relate the results of the drag coefficient, the flow visualization test has been conducted. since the delay of separation point and lower wake recirculation length results in a lower drag coefficient for the cylinders. Figures 5a through 5d show the flow separation point with the red arrows indicating the start of the flow separation point. It can be seen clearly that the effect of the grooves in delaying the separation point is effective noting that the recirculation length of the smooth cylinder is much longer compared to the other cylinders (with grooves). The full-grooved cylinder showed the shortest recirculation length in which this result is in good agreement with the one reported in [4]. Note that the flow visualization test was run in parallel with the drag and lift coefficient tests.



(a)

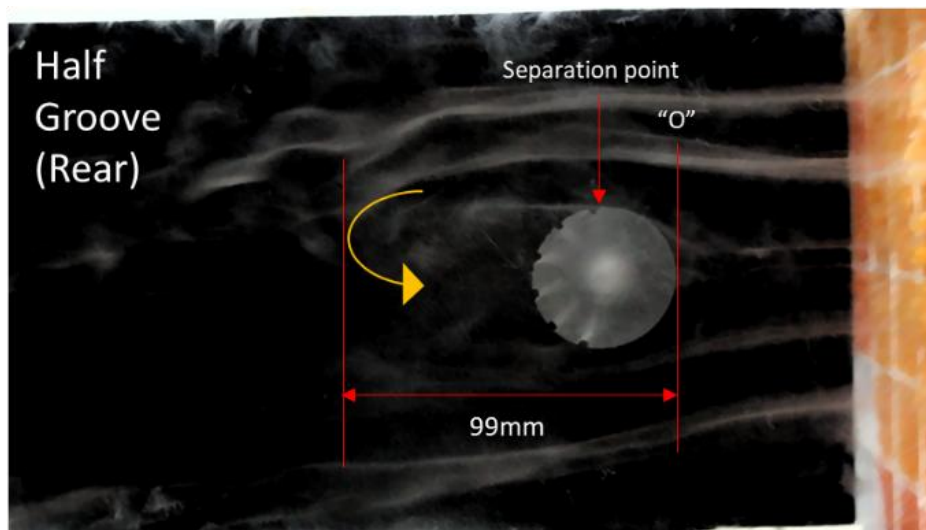
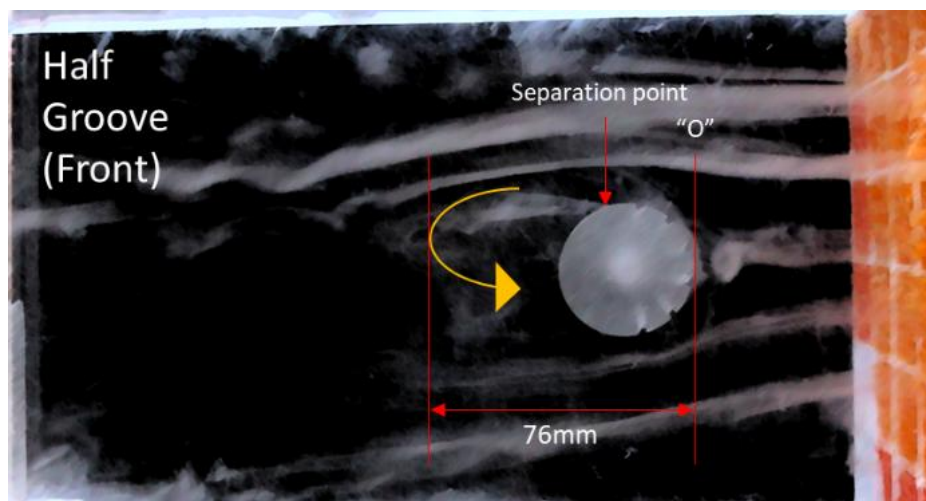
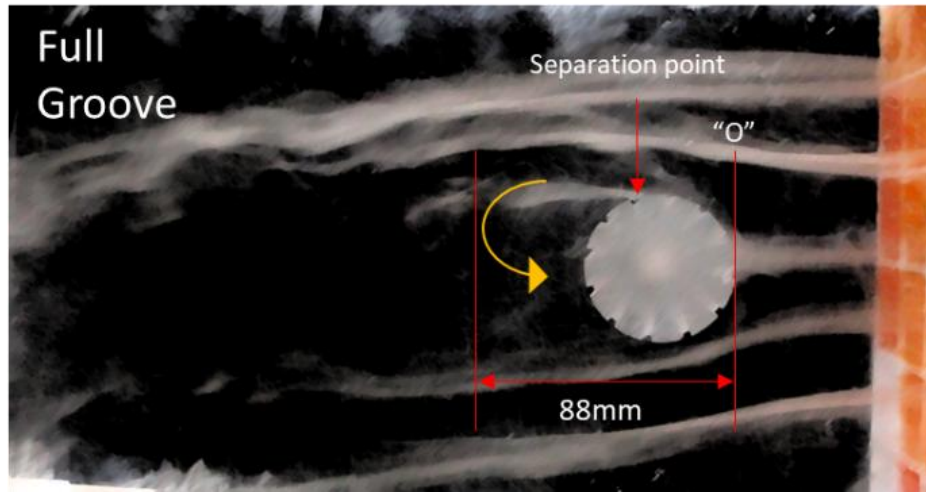


Figure 5: Flow visualization test results (a) smooth cylinder (b) full-grooved cylinder (c) half-grooved cylinder (front) (d) half-grooved cylinder (rear)

4.0 CONCLUSION

This study presents the analyzed results on the effect of grooves on the drag and lift coefficient values. Three cylinder models consisting of the smooth, half-grooved and full-grooved cylinders were tested. The experiment was conducted at a low speed open end wind tunnel with two different orientations on the half-grooved cylinder. The result indicates that grooved cylinder is effective in reducing the drag and lift coefficients on the cylinder especially for the flow having higher *Reynolds* number. The full-grooved cylinder showed the highest reduction value followed by the half-grooved located on the streamside followed by the half-grooved located at the leeside and finally the smooth cylinder. This is consistent with the smoke visualization results that the grooved surface roughness reduces the cylinder wake recirculation length. The smoke visualization also indicates that the separation point on the grooved cylinder further results in narrower wake size.

REFERENCES

1. Butt U. and Egbers C., 2013. Aerodynamic Characteristics of Flow over Circular Cylinders with Patterned Surface, *International Journal of Materials, Mechanics and Manufacturing*, 1(2): 121-125.
2. Guven O., Farrell C. and Patel V.C., 1980. Surface-roughness Effects on the Mean Flow Past Circular Cylinders, *Journal of Fluid Mechanics*, 98(4): 673-701.
3. Bearman P.W. and Harvey J.K., 1993. Control of Circular Cylinder Flow by the Use of Dimples, *AIAA Journal*, 31(10): 1753.
4. Zhou B., Wang X., Guo W., Gho W.M. and Tan S.K., 2015. Experimental Study on Flow Past a Circular Cylinder with Rough Surface, *Ocean Engineering*, 109: 7-13.
5. Dandan M.A., Samion S., Musa M.N. and Zawawi F.M., 2019. Evaluation of Lift and Drag Force of Outward Dimple Cylinder Using Wind Tunnel, *CFD Letters*, 11(3): 145-153.
6. Song X., Qi Y., Zhang M., Zhang G. and Zhan W., 2019. Application and Optimization of Drag Reduction Characteristics on the Flow Around a Partial Grooved Cylinder by Using the Response Surface Method, *Engineering Applications of Computational Fluid Mechanics*, 13(1): 158-176.
7. Kimura T. and Tsutaharat M., 1991. Fluid Dynamic Effects of Grooves on Circular Cylinder Surface, *AIAA Journal*, 29(12): 2062-2068.
8. Yamagishi Y. and Oki M., 2004. Effect of Groove Shape on Fluid Flow around a Circular Cylinder with Grooves, *Journal of Visualization*, 7: 209-216.
9. Quintavalla S.J., Angilella A.J. and Smits A.J., 2013. Drag Reduction on Grooved Cylinders in the Critical Reynolds Number Regime, *Experimental Thermal and Fluid Science*, 48: 15-18.
10. Doreti L.K. and Dineshkumar L., 2018. Control Techniques in Flow Past a Cylinder- A Review, *IOP Conferenc Series Material Science Engineering*, 377: 12144.
11. Lim H. and Lee S.J., 2002. Flow Control of Circular Cylinders with Longitudinal Grooved Surfaces, *AIAA Journal*, 40(10): 2027-2036.
12. Huang S., 2010. Cylinder Drag Reduction by the Use of Helical Grooves, *Proceedings of the HYDRALAB III Joint User Meeting*, Hannover, 2005-2008.
13. Schlichting H. and Gersten K., 2016. *Boundary-layer Theory*, Springer.
14. Çengel Y.A. and Cimbala J.M., 2013. *Fluid Mechanics: Fundamentals and Applications*, McGraw-Hill Education.